Radiation from a Circular Loop in the Presence of Spherically Symmetric Conducting or Dielectric Objects

Hakan P. Partal, *Student Member, IEEE*, Joseph R. Mautz, *Senior Member, IEEE*, and Ercument Arvas, *Senior Member, IEEE*

***Abstract*—The problem of electromagnetic radiation from a circular loop antenna of radius a, carrying a current I is considered. The loop may be radiating in the presence of one or more of the following objects: a centrally located dielectric or perfectly conducting sphere of radius $b < a$, a spherical dielectric shell of inner radius $c > a$ and outer radius d, a perfectly conducting spherically symmetric cap at radius b, and another such cap at radius d. Typical geometric structures considered are shown in Fig. 1. It is demonstrated how the presence of the sphere, shell, and caps can change and direct the radiation pattern of the loop.**

***Index Terms*—Circular loop, dielectric bodies, loop antennas, radomes, spheres, spherical antennas.**

I. Introduction

THE electromagnetic field of a circular loop antenna in free-space has been widely investigated [1]–[4] (see also the references listed in [4]). Circular loops radiating in the presence of dielectric material were studied. Examples are the insulated loops [5], [6], the loop near a planar interface [7], [8], and the loop near a model of the side of a human head [9]. The effect of a perfectly conducting open spherical shell on the field not of a loop but of a plane wave was treated in [10] and [11]. The effect of perfectly conducting spherical caps on the field of a loop was considered in [12]. In [13], spherically symmetric dielectrics were used to modify the radiation pattern of a loop.

Consider the field of a circular loop antenna near symmetrically placed spherical dielectric and/or perfectly conducting objects. These objects can be used to shape the radiation pattern of the loop of radius a. The particular dielectric and conducting objects used are a centrally located dielectric or conducting sphere of radius $b < a$, perfectly conducting spherical caps of radii $b < a$ and $c > a$, and a dielectric shell of inner radius c and outer radius d. Radiation patterns are obtained for the three cases shown in Fig. 1.

The field of the circular loop radiating in any one of the three environments shown in Fig. 1 is expressed as the field of an electric vector potential $\mathbf{a}_r F_r$ where $\mathbf{a}_r$ is the unit vector in the radial direction from the origin at the center of the loop and $F_r = r\psi$ where r is the distance from the origin and ψ is a solution to the Helmholtz equation ([14], (6–26)). Due to symmetry, there is no radially directed magnetic vector potential and F_r does not depend on the angle ϕ shown Fig. 1(c). For $r < b, F_r$ is constructed to be finite at the origin. For each of regions $b < r < a, a < r < c$, and $c < r < d, F_r$ consists of both inward and outward traveling waves, and F_r consists of only outward traveling waves in the region where $r > d$. The exact solution requires an infinite number of waves in each region so that F_r must have an infinite series representation in each of the five regions.

We retain only the first M terms of the infinite series representation of F_r in each region. For all cases shown in Fig. 1, all boundary conditions except those at $r = a$ are that the tangential electric and magnetic fields are continuous at all dielectric interfaces and that the tangential electric field vanishes on the surface of the conducting sphere and on each side of each conducting cap. At $r = a$, the tangential electric field is continuous and, with the electric current I of the loop viewed as the electric current density $\mathbf{a}_\phi J_\phi$ on the surface of the sphere of radius a, the θ component of the magnetic field suddenly increases by J_ϕ as r passes through a in the direction of increasing r. Here, $\mathbf{a}_\phi$ is the unit vector in the ϕ direction and

$$J_\phi = (I/a)\delta(\theta - \pi/2)$$

where δ is the Dirac delta function.

II. Formulation

We want to obtain the far-field patterns for the three cases shown in Fig. 1. In Case (a) shown in Fig. 1(a), the loop of radius a carrying the electric current $I(\phi)$ radiates in the presence of a dielectric sphere of radius $b < a$ and relative permittivity ε_1 and a dielectric shell $(c < r < d)$ of relative permittivity ε_2. Here, r is the distance from the center of the loop. In Case (b) shown in Fig. 1(b), the loop radiates in the presence of a conducting cap for $0 < \theta < \theta_1$ at $r = b < a$ and a conducting cap for $\theta_2 < \theta < \pi$ at $r = d > a$. In Case (c) shown in Fig. 1(c), the loop radiates in the presence of a dielectric or conducting sphere of radius $b < a$, a dielectric shell $(c < r < d)$, and a conducting cap $(\theta_1 < \theta < \theta_2)$ at $r = d$.

Manuscript received September 7, 1999; revised March 6, 2000. This work was supported in part by the CASE Center at Syracuse University.

The authors are with the Department of Electrical Engineering and Computer Science, Syracuse University, Syracuse, NY 13244 USA (e-mail: earvas@syr.edu).

Publisher Item Identifier S 0018-926X(00)09369-8.

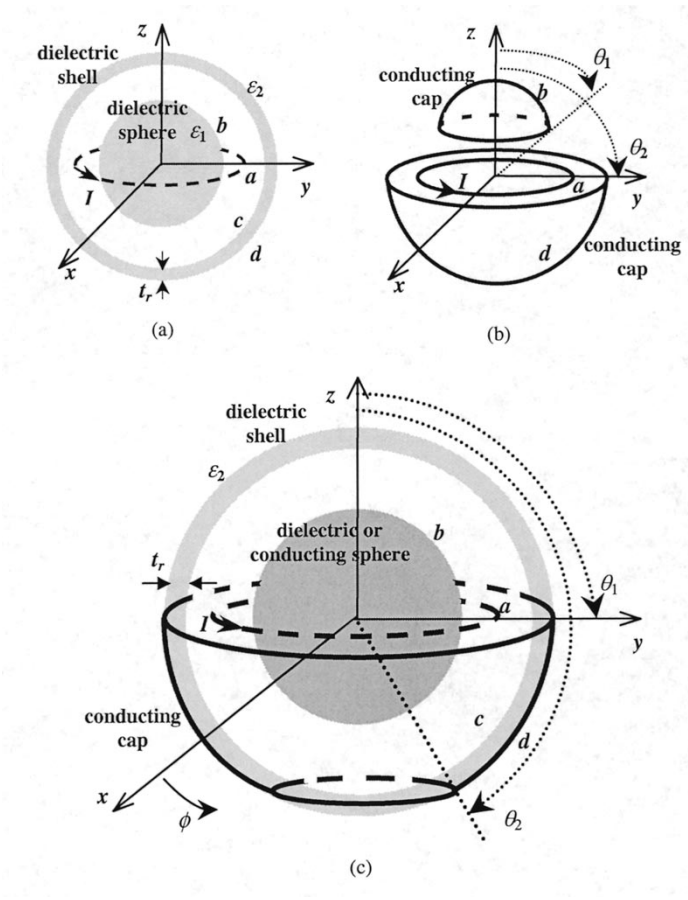

Fig. 1. Typical cases considered. (a) Dielectric sphere inside the loop and radome outside. (b) Conducting caps at $r = b < a$ and $r = d > a$. (c) Dielectric and conducting objects around the loop.

In practice, the loop is driven by a voltage source at one point on the loop, resulting in nonuniform loop current when the radius of the loop is one wavelength or more. In that case, the current can be expanded into an even Fourier series as follows.

$$I(\phi) = I_0 + I_1 \cos\phi + I_2 \cos(2\phi) + I_3 \cos(3\phi) \cdots. \quad (1)$$

In this paper, the contribution due to the constant term is computed. Moreover, an almost uniform current may be obtained by multiple feeds and the results presented in our paper will be valid for such excitation.

If the excitation is distributed, radiation resistance is not clearly defined because there is no clearly defined reference current. For this reason, no radiation resistances were computed.

Due to symmetry, the electric field has no radial component so that the electromagnetic field can be obtained from an electric vector potential $\mathbf{a}_r F_r$ where $\mathbf{a}_r$ is the unit vector in the radial direction and F_r is given by (2), shown at the bottom of the page where P_n is the Legendre polynomial of degree n. Also, $\hat{J}_n, \hat{H}_n^{(1)}$, and $\hat{H}_n^{(2)}$ are the alternative spherical Bessel functions ([14], Appendix D), and $a_n, b_n, c_n, d_n, e_n, f_n, g_n$, and h_n are constants to be determined. Furthermore, k_1 is the wavenumber in the region where $r < b, k_2$ is the wavenumber in the region where $c < r < d$, and k is the wavenumber in the rest of space. In the exact solution, $M = \infty$. The approximate solutions presented in this paper were calculated with $M = 40$. The electric and magnetic fields obtained from F_r are respectively $\mathbf{E} = \mathbf{a}_\phi E_\phi$ and $\mathbf{H} = \mathbf{a}_r H_r + \mathbf{a}_\theta H_\theta$ where [14, (6)–(26)]

$$E_\phi = \frac{1}{r}\frac{\partial F_r}{\partial \theta} \quad (3)$$

and

$$H_\theta = \frac{1}{j\omega\mu r}\frac{\partial^2 F_r}{\partial r \partial \theta}. \quad (4)$$

Here, $\mathbf{a}_r, \mathbf{a}_\theta$, and $\mathbf{a}_\phi$ are the unit vectors in the r, θ, and ϕ directions, respectively. Also, ω is the angular frequency and μ is the permeability. The field component H_r is not needed because we will not impose any boundary conditions on it.

Case (a) is treated in this paragraph and the next four. At $r = a, E_\phi$ is continuous for all θ and, assuming that the constant loop current is expressed as $\mathbf{a}_\phi J_\phi$, H_θ has a discontinuity equal to J_ϕ

$$d_n \hat{H}_n^{(1)}(ka) + e_n \hat{H}_n^{(2)}(ka) - b_n \hat{H}_n^{(1)}(ka) - c_n \hat{H}_n^{(2)}(ka) = 0 \quad (5)$$

$$H_\theta(r = a^+) - H_\theta(r = a^-) = J_\phi = \frac{I_0}{a}\delta(\theta - \pi/2) \quad (6)$$

where $r = a^+$ and $r = a^-$ denote the limits as r approaches a from above and below respectively. In view of (2), substitution of (4) into (6) gives

$$j\eta I_0 \delta(\theta - \pi/2) = \sum_{n=1}^{M} \frac{d}{d\theta} P_n(\cos\theta) \times \left[d_n \hat{H}_n^{(1)\prime}(ka) + e_n \hat{H}_n^{(2)\prime}(ka) - b_n \hat{H}_n^{(1)\prime}(ka) - c_n \hat{H}_n^{(2)\prime}(ka) \right] \quad (7)$$

$$F_r = \lim_{M\to\infty} \begin{cases} \sum_{n=1}^{M} P_n(\cos\theta) a_n \hat{J}_n(k_1 r), & r < b \\ \sum_{n=1}^{M} P_n(\cos\theta) \left[b_n \hat{H}_n^{(1)}(kr) + c_n \hat{H}_n^{(2)}(kr) \right], & b < r < a \\ \sum_{n=1}^{M} P_n(\cos\theta) \left[d_n \hat{H}_n^{(1)}(kr) + e_n \hat{H}_n^{(2)}(kr) \right], & a < r < c \\ \sum_{n=1}^{M} P_n(\cos\theta) \left[f_n \hat{H}_n^{(1)}(k_2 r) + g_n \hat{H}_n^{(2)}(k_2 r) \right], & c < r < d \\ \sum_{n=1}^{M} P_n(\cos\theta) h_n \hat{H}_n^{(2)}(kr), & r > d \end{cases} \quad (2)$$

where η is the intrinsic impedance of free-space. Multiplying both sides of (7) by $(dP_q/dP_\theta)\sin\theta$, then integrating from 0 to π, and next using [15, p. 489]

$$\int_0^\pi \frac{dP_n}{d\theta}\frac{dP_q}{d\theta}\sin\theta\,d\theta = \delta_{nq}\frac{2n(n+1)}{2n+1}, \qquad \delta_{nq} = \begin{cases} 1, & n=q \\ 0, & n\neq q \end{cases} \tag{8}$$

and [14, (E-25), (E-27)]

$$\left[\frac{dP_n(\cos\theta)}{d\theta}\right]_{\theta=\pi/2} = \left[P_n^1(\cos\theta)\right]_{\theta=\pi/2} = P_n^1(0) = \begin{cases} 0, & n \text{ even} \\ (-1)^{(n+1)/2}\frac{1\cdot3\cdot5\cdots n}{2\cdot4\cdot6\cdots(n-1)}, & n \text{ odd} \end{cases} \tag{9}$$

we obtain, upon replacement of q by n,

$$d_n\hat{H}_n^{(1)\prime}(ka) + e_n\hat{H}_n^{(2)\prime}(ka) - b_n\hat{H}_n^{(1)\prime}(ka) - c_n\hat{H}_n^{(2)\prime}(ka) = T_n \tag{10}$$

where T_n is given in the Appendix.

Continuity of E_ϕ at $r=b$, continuity of E_ϕ at $r=c$, continuity of H_θ at $r=c$, and continuity of E_ϕ at $r=d$ are expressed as

$$b_n\hat{H}_n^{(1)}(kb) + c_n\hat{H}_n^{(2)}(kb) - a_n\hat{J}_n(k_1b) = 0 \tag{11}$$

$$f_n\hat{H}_n^{(1)}(k_2c) + g_n\hat{H}_n^{(2)}(k_2c) - d_n\hat{H}_n^{(1)}(kc) - e_n\hat{H}_n^{(2)}(kc) = 0 \tag{12}$$

$$f_n\hat{H}_n^{(1)\prime}(k_2c) + g_n\hat{H}_n^{(2)\prime}(k_2c) - \frac{\eta^2}{\eta}\left(d_n\hat{H}_n^{(1)\prime}(kc) + e_n\hat{H}_n^{(2)\prime}(kc)\right) = 0 \tag{13}$$

$$h_n\hat{H}_n^{(2)}(kd) - f_n\hat{H}_n^{(1)}(k_2d) - g_n\hat{H}_n^{(2)}(k_2d) = 0 \tag{14}$$

where η_2 is the intrinsic impedance in the dielectric shell.

Continuity of H_θ at $r=b$ and continuity of H_θ at $r=d$ are expressed as:

$$\frac{\eta_1}{\eta}\left[b_n\hat{H}_n^{(1)\prime}(kb) + c_n\hat{H}_n^{(2)\prime}(kb)\right] - a_n\hat{J}_n{}'(k_1b) = 0 \tag{15}$$

$$f_n\hat{H}_n^{(1)\prime}(k_2d) + g_n\hat{H}_n^{(2)\prime}(k_2d) - \frac{\eta_2}{\eta}h_n\hat{H}_n^{(2)\prime}(kd) = 0 \tag{16}$$

where η_1 is intrinsic impedance in the dielectric sphere.

Equations (5) and (10)–(16) constitute a system of eight simultaneous equations involving the eight unknown coefficients $a_n, b_n, c_n, d_n, e_n, f_n, g_n$, and h_n. This system is solved for h_n by first obtaining two equations involving only the unknowns b_n and h_n and then solving these two equations for h_n. The two equations involving only the two unknowns b_n and h_n are obtained by first using the two equations at $r=b$ to solve for c_n in terms of b_n, then using the two equations at $r=a$ to solve for d_n and e_n in terms of b_n and c_n. Next, the previously found expression for c_n is used to express d_n and e_n in terms of only b_n. Then, the two equations at $r=c$ are used to solve for f_n and g_n in terms of d_n and e_n. Next, the previously found expressions for d_n and e_n are used to express f_n and g_n in terms of only b_n. These expressions are substituted into the two equations at $r=d$. Finally, these two equations, which now involve only the unknowns h_n and b_n, are solved for h_n. The procedure described in the previous seven sentences is implemented by first using (11) and (15) to obtain

$$c_n = K_{cb}b_n \tag{17}$$

where K_{cb} is given in the Appendix. Then, (5) and (10) are used to obtain

$$d_n = b_n - \frac{j}{2}\hat{H}_n^{(2)}(ka)T_n \tag{18}$$

$$e_n = c_n + \frac{j}{2}\hat{H}_n^{(1)}(ka)T_n. \tag{19}$$

Substitution of (17) into (19) gives

$$e_n = K_{cb}b_n + \frac{j}{2}\hat{H}_n^{(1)}(ka)T_n. \tag{20}$$

Next, (12) and (13) are used to obtain

$$f_n = K_{fd}d_n + K_{fe}e_n \tag{21}$$

$$g_n = K_{gd}d_n + K_{ge}e_n \tag{22}$$

where the K's are given in the Appendix. Substitution of (18) and (20) into (21) and (22) gives

$$f_n = K_{fb}b_n + K_{fo} \tag{23}$$

$$g_n = K_{gb}b_n + K_{go} \tag{24}$$

where the K's are given in the Appendix. Substituting (23) and (24) into (14) and (16), we obtain

$$h_n\hat{H}_n^{(2)}(kd) = K_{hb}b_n + K_{ho} \tag{25}$$

$$\frac{\eta_2}{\eta}h_n\hat{H}_n^{(2)\prime}(kd) = K'_{hb}b_n + K'_{ho} \tag{26}$$

where the K's and K''s are given in the Appendix. Solving (25) and (26) for h_n, we obtain

$$h_n = \frac{K'_{hb}K_{ho} - K_{hb}K'_{ho}}{K'_{hb}\hat{H}_n^{(2)}(kd) - \frac{\eta_2}{\eta}K_{hb}\hat{H}_n^{(2)\prime}(kd)}. \tag{27}$$

For $r > d$,

$$E_\phi = \frac{1}{r}\sum_{n=1}^{M} h_n\hat{H}_n^{(2)}(kr)\frac{d}{d\theta}P_n(\cos\theta) \tag{28}$$

In the far zone where ([14], (D-24))

$$\hat{H}_n^{(2)}(kr) = j^{n+1}e^{-jkr}, \tag{29}$$

(28) reduces to

$$E_\phi = \frac{e^{-jkr}}{r}\sum_{n=1}^{M} j^{n+1}h_n\frac{d}{d\theta}P_n(\cos\theta). \tag{30}$$

In Case (b), where the conducting caps are at $r=b$ and $r=d$, the region for which $c<r<d$ is "squeezed out" and the unknown coefficients f_n and g_n that appeared in the expression for the electric vector potential in this region in Case (a) are also "squeezed out". Equations (5) and (10) are valid as they stand,

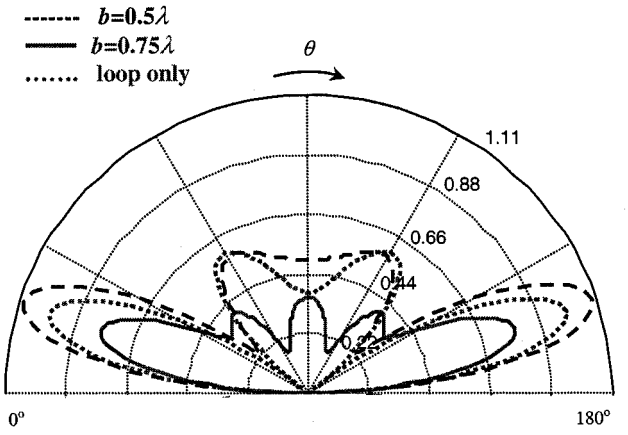

(a)

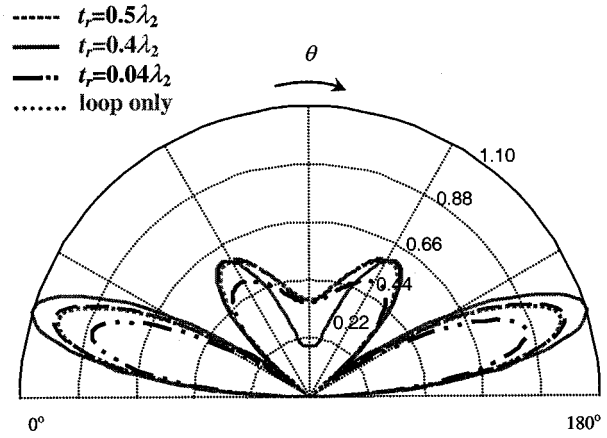

(b)

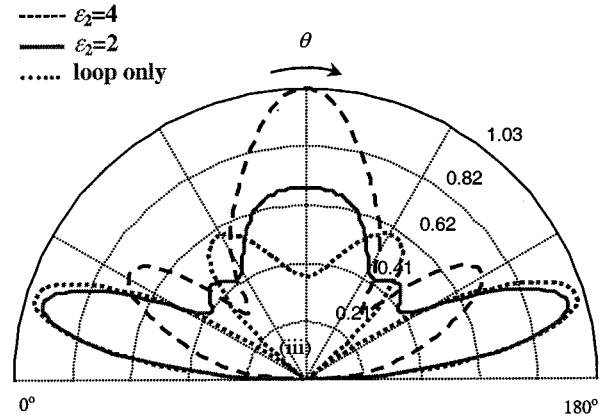

(c)

Fig. 2. Far-field patterns in the presence of dielectric bodies [Case (a)]. (a) A dielectric sphere of radius b, and $\varepsilon_1 = 4.0$ inside the loop. (b) A radome of inner radius $c = 3.0\ \lambda$, and $\varepsilon_2 = 4.0$ surrounding the loop. (c) A dielectric sphere inside the loop and a radome surrounding the loop for $b = 0.5\ \lambda, c = 1.2\ \lambda, d = 1.3\ \lambda$, and $\varepsilon_1 = 4$.

(11) is valid with k_1 replaced by k, and (14) is valid with f_n, g_n, and k_2 replaced by d_n, e_n, and k, respectively:

$$b_n\hat{H}_n^{(1)}(kb) + c_n\hat{H}_n^{(2)}(kb) - a_n\hat{J}_n(kb) = 0 \quad (31)$$

$$h_n\hat{H}_n^{(2)}(kd) - d_n\hat{H}_n^{(1)}(kd) - e_n\hat{H}_n^{(2)}(kd) = 0. \quad (32)$$

Setting $E_\phi = 0$ for $0 < \theta < \theta_1$ at $r = b$ and enforcing continuity of H_θ for $\theta_1 < \theta < \pi$ at $r = b$, we obtain

$$\sum_{n=1}^{M} \frac{d}{d\theta}P_n(\cos\theta)a_n\hat{J}_n(kb) = 0, \quad 0 < \theta < \theta_1 \quad (33)$$

$$\sum_{n=1}^{M} \frac{d}{d\theta}P_n(\cos\theta)\left\{b_n\hat{H}_n^{(1)\prime}(kb) + c_n\hat{H}_n^{(2)\prime}(kb) - a_n\hat{J}_n'(kb)\right\} = 0, \quad \theta_1 \le \theta \le \pi. \quad (34)$$

Enforcing continuity of H_θ for $0 < \theta < \theta_2$ at $r = d$ and setting $E_\phi = 0$ for $\theta_2 < \theta < \pi$ at $r = d$, we obtain

$$\sum_{n=1}^{M} \frac{d}{d\theta}P_n(\cos\theta)\left\{d_n\hat{H}_n^{(1)\prime}(kd) + e_n\hat{H}_n^{(2)\prime}(kd) - h_n\hat{H}_n^{(2)\prime}(kd)\right\} = 0, \quad 0 < \theta < \theta_2 \quad (35)$$

$$\sum_{n=1}^{M} \frac{d}{d\theta}P_n(\cos\theta)h_n\hat{H}_n^{(2)}(kd) = 0, \quad \theta_2 < \theta < \pi. \quad (36)$$

Equations (33) and (34) complement each other to form a single mixed boundary value equation. Similarly, (35) and (36) form another mixed boundary value equation. First using (31), and then using (5) and (10), we express c_n, d_n, and e_n in terms of a_n and b_n. Using (32) to eliminate b_n in favor of h_n in our expressions for c_n, d_n, and e_n, we express b_n, c_n, d_n, and e_n in terms of a_n and h_n. Substituting these newly found expressions into (33)–(36), we obtain

$$\sum_{n=1}^{M} \frac{d}{d\theta}P_n(\cos\theta)a_n\hat{J}_n(kb) = 0, \quad 0 < \theta < \theta_1 \quad (37)$$

$$\sum_{n=1}^{M} \frac{d}{d\theta}P_n(\cos\theta)\frac{1}{K_{dd}}\left[-2\hat{J}_n(kd)a_n + 2\hat{H}_n^{(2)}(kd)h_n + jK_{T1}T_n\right] = 0, \quad \theta_1 < \theta < \pi \quad (38)$$

and

$$\sum_{n=1}^{M} \frac{d}{d\theta}P_n(\cos\theta)\frac{1}{K_{dd}}\left[-2\hat{J}_n(kb)a_n + 2\hat{H}_n^{(2)}(kb)h_n + jK_{T2}T_n\right] = 0, \quad 0 < \theta < \theta_2 \quad (39)$$

$$\sum_{n=1}^{M} \frac{d}{d\theta}P_n(\cos\theta)h_n\hat{H}_n^{(2)}(kd) = 0, \quad \theta_2 < \theta < \pi \quad (40)$$

where T_n, K_{dd}, K_{T1}, and K_{T2} are given in the Appendix.

Enforcing the composite equation consisting of (37) and its complement (38) at M equally spaced values of θ between 0 and π and enforcing the composite equation consisting of (39) and

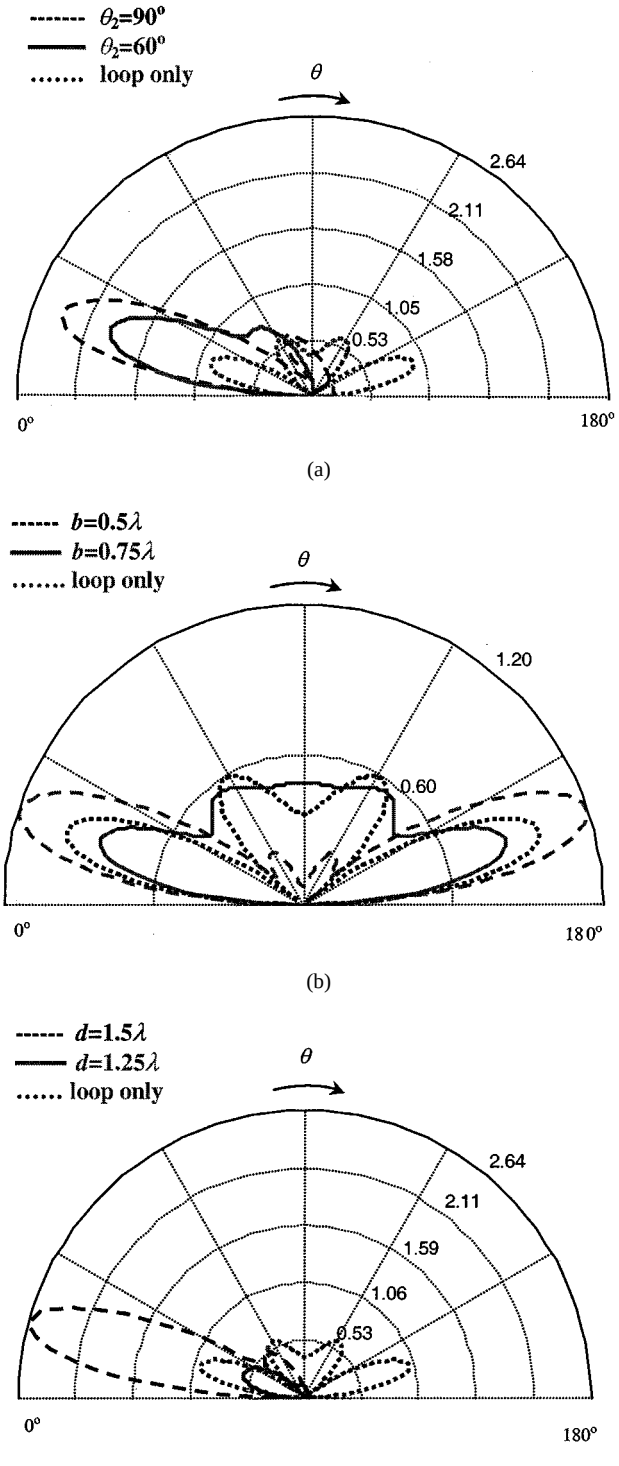

Fig. 3. Far-field patterns in the presence of conducting bodies [Case (b)]. (a) One conducting cap at $r = d = 1.5\ \lambda$. (b) One complete sphere of radius b inside the loop. (c) A conducting cap at $r = b$ and another conducting cap at $r = d$ for $\theta_1 = 90°, \theta_2 = 90°$, and $b = 0.5\ \lambda$.

its complement (40) at the same values of θ, we obtain $2M$ equations involving the $2M$ unknowns $\{a_n, h_n, n = 1, 2, \ldots, M\}$. In the far zone, E_ϕ is given by (30) where h_n is the solution of these $2M$ equations.

In Case (c), (5), (10), and (12)–(14) hold. If the sphere is dielectric, (11) and (15) hold. If the sphere is conducting, then the tangential electric field is zero at $r = b$ so that (11) holds with $a_n = 0$:

$$b_n \hat{H}_n^{(1)}(kb) + c_n \hat{H}_n^{(2)}(kb) = 0. \tag{41}$$

Continuity of tangential magnetic field at $r = d$ for $0 < \theta < \theta_1$ and $\theta_2 < \theta < \pi$ gives

$$\sum_{n=1}^{M} \frac{d}{d\theta} P_n(\cos\theta) \left[f_n \hat{H}_n^{(1)\prime}(k_2 d) + g_n \hat{H}_n^{(2)\prime}(k_2 d) - \frac{\eta_2}{\eta} h_n H_n^{(2)\prime}(kd) \right] = 0, \quad \begin{cases} 0 < \theta < \theta_1 \\ \theta_2 < \theta < \pi \end{cases}. \tag{42}$$

Setting the tangential electric field equal to zero at $r = d$ for $\theta_1 < \theta < \theta_2$, we have

$$\sum_{n=1}^{M} \frac{d}{d\theta} P_n(\cos\theta) h_n \hat{H}_n^{(2)}(kd) = 0, \quad \theta_1 < \theta < \theta_2. \tag{43}$$

Equations (42) and (43) complement each other to form one composite equation.

In Case (c), (17)–(25) are valid where K_{cb} is given by (A.2) if the sphere is dielectric and by (A.18) if the sphere is conducting. Substituting into (23) and (24) the solution of (25) for b_n in terms of h_n, we obtain

$$f_n = \frac{K_{fb}\left(\hat{H}_n^{(2)}(kd) h_n - K_{ho}\right)}{K_{hb}} + K_{fo} \tag{44}$$

$$g_n = \frac{K_{gb}\left(\hat{H}_n^{(2)}(kd) h_n - K_{ho}\right)}{K_{hb}} + K_{go}. \tag{45}$$

With f_n and g_n given by (44) and (45), (42) and (43) are seen to be one composite equation involving the M unknowns $h_1, h_2, \ldots, h_M$. If instead of the single conducting cap shown in Fig. 1(c), there are two conducting caps at $r = d$, one extending from $\theta_1 < \theta < \theta_2$, and the other extending from $\theta_3 < \theta < \theta_4$, then the domain of (42) changes to $(0 < \theta < \theta_1, \theta_2 < \theta < \theta_3, \theta_4 < \theta < \pi)$ and the domain of (43) changes to $(\theta_1 < \theta < \theta_2, \theta_3 < \theta < \theta_4)$.

Enforcing the composite equation described in the previous paragraph at M equally spaced values of θ between zero and π, we obtain M equations involving the M unknown h's. In the far zone, E_ϕ is given by (30) where h_n is the solution of these M equations.

III. Numerical Results and Discussion

For various purposes, conducting or dielectric objects can be located near a circular loop antenna to change or direct the radiation pattern. All far-field patterns shown in Figs. 2–4 are plots of $|E_\phi|_{\text{norm}}$ where, with regard to (30),

$$|E_\phi|_{\text{norm}} = \frac{1}{\alpha} \left| \sum_{n=1}^{M} j^{n+1} h_n \frac{d}{d\theta} P_n(\cos\theta) \right| \tag{46}$$

where the right-hand side of (46) was calculated by taking the uniform loop current to be $I_0 = 10$ mA on a loop of radius λ where λ is the wavelength in free-space. The constant α was chosen to render the maximum value of the computed right-hand

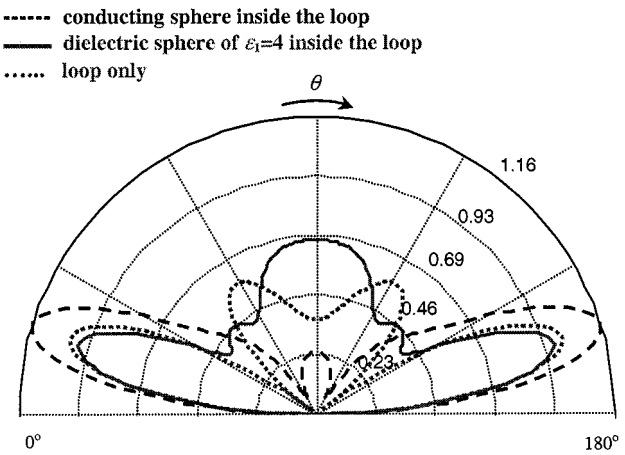

(a)

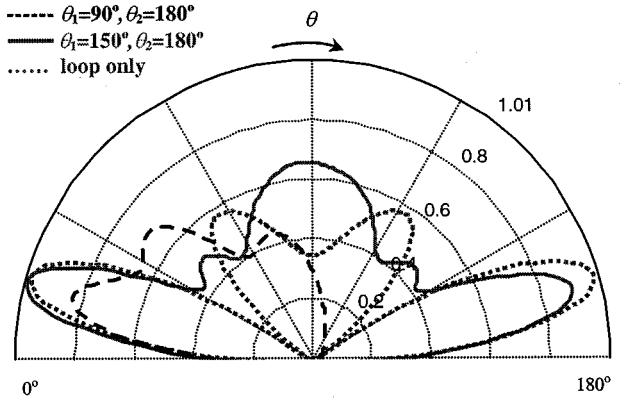

(b)

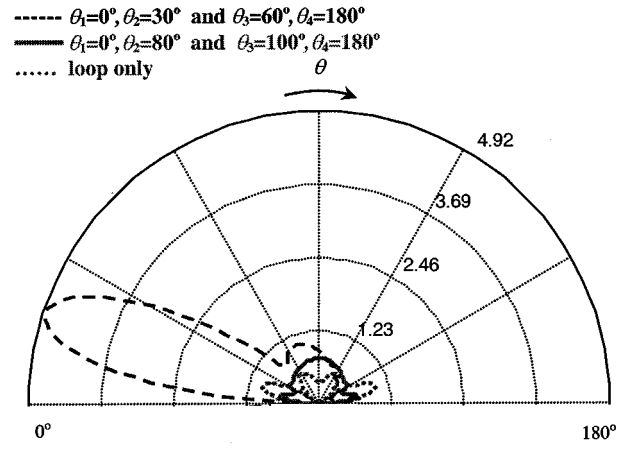

(c)

Fig. 4. Far-field patterns in the presence of dielectric and conducting bodies [Case (c)]. (a) A dielectric or conducting sphere inside the loop and a radome surrounding the loop for $b = 0.5\ \lambda, \varepsilon_2 = 2, c = 1.2\ \lambda, d = 1.3\ \lambda$. (b) A dielectric sphere inside the loop, and a conducting cap on the outside surface of the radome for $b = 0.5\ \lambda, \varepsilon_1 = 4, \varepsilon_2 = 2, c = 1.2\ \lambda, d = 1.3\ \lambda$. (c) A conducting sphere inside the loop, a radome surrounding the loop, and a two-piece conducting cap on the outside surface of the radome for $b = 0.75\ \lambda, \varepsilon_2 = 2, c = 1.2\ \lambda, d = 1.3\ \lambda$ (unlike the one-piece cap that covers $\theta_1 < \theta < \theta_2$ in Fig. 1(c), the two-piece cap covers both $\theta_1 < \theta < \theta_2$, and $\theta_3 < \theta < \theta_4$ where $0^\circ \leq \theta_1 < \theta_2 < \theta_3 < \theta_4 \leq 180^\circ$).

side of (46) unity for the loop radiating in free-space. So chosen, $\alpha = 6.8913$ volts.

A dielectric sphere of radius $b < a$ will change the shape of the radiation pattern of the loop depending on the permittivity of the sphere and its radius (see Fig. 2(a)). While a dielectric shell (radome) of inner radius $c > a$ and outer radius d protects the antenna from environmental effects, it could change the radiation pattern considerably. However, when the thickness $t_r = \lambda_2/2$ where λ_2 is the wavelength in the radome, the field of the loop antenna seems to pass through the radome without much alteration as seen in Fig. 2(b). In Fig. 2(c), the effect of both dielectric spheres inside the loop and radome outside can be seen as the relative permittivity of the radome increases. A radome whose thickness t_r is small in Figs. 2(b) and 2(c) can be approximated by a $1/j\omega\varepsilon_0(\varepsilon_2 - 1)t_r$ ohm impedance sheet [16] where ε_0 is the absolute permittivity of free-space and ε_2 is the relative permittivity of the radome. We have used this approximation which resulted in one less unknown coefficient. The approximate results so obtained were observed to be in excellent agreement with the exact results when $t_r < 0.1\lambda_2$.

In Fig. 3(a), a conducting cap at $r = d$ behind the loop enhances the two forward lobes and degrades the two backward lobes. The enhancement and degradation are most pronounced when the cap is hemispherical and $d - a = \lambda/2$. In Fig. 3(b), a conducting sphere of radius $b < a$ enhances the radiation at $\theta = 90^\circ$ when $a - b = \lambda/4$ but enhances the main lobes and degrades the radiation at and near $\theta = 90^\circ$ when $a - b = \lambda/2$. In Fig. 3(c), conducting caps at $r = b$ and $r = d$ serve to enhance the two forward lobes when $d - a = \lambda/2$.

In Fig. 4(a), the loop radiates in the presence of a conducting or dielectric sphere inside as well as a thin radome outside. Figure 4(b) shows radiation patterns of the loop in the presence of a dielectric sphere inside and a radome as well as a conducting cap outside. The loop whose patterns appear in Fig. 4(c) radiates in the presence of a conducting sphere inside and a radome outside with two conducting caps on its outside surface. One cap extends from $\theta = \theta_1$ to $\theta = \theta_2$, and the other extends from $\theta = \theta_3$ to $\theta = \theta_4$. The two main lobes are greatly enhanced when $a - b = \lambda/4, \theta_1 = 0^\circ, \theta_2 = 30^\circ, \theta_3 = 60^\circ$, and $\theta_4 = 180^\circ$, that is, when radiation can only escape from the part of the outside surface of the radome for which $30^\circ < \theta < 60^\circ$.

IV. Conclusion

Radiation patterns of a circular loop of electric current in the presence of spherically symmetric conducting or dielectric objects were computed. The presence of such objects could change the radiation pattern of the loop current appreciably. However, their effect on the pattern is very complicated.

Appendix

In (10)

$$T_n = \begin{cases} 0, & n \text{ even} \\ j\eta I_0(-1)^{(n+1)/2} \frac{(2n+1)}{2n} \frac{1\cdot 3\cdot 5 \cdots n}{2\cdot 4\cdot 6 \cdots (n+1)}, & n \text{ odd} \end{cases} \tag{A.1}$$

In (17)

$$K_{cb} = \frac{\hat{J'}_n(k_1 b)\hat{H}_n^{(1)}(kb) - \frac{\eta_1}{\eta}\hat{J}_n(k_1 b)\hat{H}_n^{(1)'}(kb)}{\frac{\eta_1}{\eta}\hat{J}_n(k_1 b)\hat{H}_n^{(2)'}(kb) - \hat{J'}_n(k_1 b)\hat{H}_n^{(2)}(kb)}. \quad \text{(A.2)}$$

In (21) and (22)

$$K_{fd} = \frac{j}{2}\hat{H}_n^{(2)'}(k_2 c)\hat{H}_n^{(1)}(kc) - \frac{\eta_2}{\eta}\hat{H}_n^{(2)}(k_2 c)\hat{H}_n^{(1)'}(kc) \quad \text{(A.3)}$$

$$K_{fe} = \frac{j}{2}\hat{H}_n^{(2)'}(k_2 c)\hat{H}_n^{(2)}(kc) - \frac{\eta_2}{\eta}\hat{H}_n^{(2)}(k_2 c)\hat{H}_n^{(2)'}(kc) \quad \text{(A.4)}$$

$$K_{gd} = \frac{-j}{2}\hat{H}_n^{(1)'}(k_2 c)\hat{H}_n^{(1)}(kc) - \frac{\eta_2}{\eta}\hat{H}_n^{(1)}(k_2 c)\hat{H}_n^{(1)'}(kc) \quad \text{(A.5)}$$

$$K_{ge} = \frac{-j}{2}\left(\hat{H}_n^{(1)'}(k_2 c)\hat{H}_n^{(2)}(kc) - \frac{\eta_2}{\eta}\hat{H}_n^{(1)}(k_2 c)\hat{H}_n^{(2)'}(kc)\right). \quad \text{(A.6)}$$

In (23) and (24)

$$K_{fb} = K_{fd} + K_{fe}K_{cb} \quad \text{(A.7)}$$

$$K_{fo} = \frac{-j}{2}T_n\left[K_{fd}\hat{H}_n^{(2)}(ka) - K_{fe}\hat{H}_n^{(1)}(ka)\right] \quad \text{(A.8)}$$

$$K_{gb} = K_{gd} + K_{ge}K_{cb} \quad \text{(A.9)}$$

$$K_{go} = \frac{-j}{2}T_n\left[K_{gd}\hat{H}_n^{(2)}(ka) - K_{ge}\hat{H}_n^{(1)}(ka)\right]. \quad \text{(A.10)}$$

In (25) and (26)

$$K_{hb} = K_{fb}\hat{H}_n^{(1)}(k_2 d) + K_{gb}\hat{H}_n^{(2)}(k_2 d) \quad \text{(A.11)}$$

$$K_{ho} = K_{fo}\hat{H}_n^{(1)}(k_2 d) + K_{go}\hat{H}_n^{(2)}(k_2 d) \quad \text{(A.12)}$$

$$K'_{hb} = K_{fb}\hat{H}_n^{(1)'}(k_2 d) + K_{gb}\hat{H}_n^{(2)'}(k_2 d) \quad \text{(A.13)}$$

$$K'_{ho} = K_{fo}\hat{H}_n^{(1)'}(k_2 d) + K_{go}\hat{H}_n^{(2)'}(k_2 d). \quad \text{(A.14)}$$

In (38) and (39), T_n is given by (A.1) and

$$K_{dd} = \hat{H}_n^{(2)}(kd)\hat{H}_n^{(1)}(kb) - \hat{H}_n^{(2)}(kb)\hat{H}_n^{(1)}(kd) \quad \text{(A.15)}$$

$$K_{T1} = \hat{H}_n^{(2)}(ka)\hat{H}_n^{(1)}(kd) - \hat{H}_n^{(2)}(kd)\hat{H}_n^{(1)}(ka) \quad \text{(A.16)}$$

$$K_{T2} = \hat{H}_n^{(2)}(kb)\hat{H}_n^{(1)}(ka) - \hat{H}_n^{(2)}(ka)\hat{H}_n^{(1)}(kb). \quad \text{(A.17)}$$

In Case (c), (A.1)–(A.12) are valid if the sphere is dielectric. If the sphere is conducting then (A.2) must be replaced by

$$K_{cb} = -\frac{\hat{H}_n^{(1)}(kb)}{\hat{H}_n^{(2)}(kb)}. \quad \text{(A.18)}$$

REFERENCES

[1] R. F. Harrington and J. Mautz, "Electromagnetic behavior of circular wire loops with arbitrary excitation and loading," *Proc. Inst. Elect. Eng.*, vol. 115, pp. 68–77, Jan. 1968.

[2] G. Zhou and G. S. Smith, "An accurate theoretical model for the thin-wire circular half-loop antenna," *IEEE Trans. Antennas Propagat.*, vol. 39, pp. 1167–1177, Aug. 1991.

[3] P. L. Overfelt, "Near fields of the constant current thin circular loop antenna of arbitrary radius," *IEEE Trans. Antennas Propagat.*, vol. 44, pp. 166–171, Feb. 1996.

[4] L. W. Li, M. S. Leong, P. S. Kooi, and T. S. Yeo, "Exact solutions of electromagnetic fields in both near and far zones radiated by thin circular-loop antennas: A general representation," *IEEE Trans. Antennas Propagat.*, vol. 45, pp. 1741–1748, Dec. 1997.

[5] J. R. Wait, "Insulated loop antenna immersed in a conducting medium," *J. Res. NBS*, vol. 59, pp. 133–137, Aug. 1957.

[6] L. N. An and G. S. Smith, "The eccentrically insulated circular loop antenna," *Radio Sci.*, vol. 15, pp. 1067–1081, Nov.–Dec. 1980.

[7] ——, "The horizontal circular loop antenna near a planar interface," *Radio Sci.*, vol. 17, pp. 483–502, May–June 1982.

[8] G. S. Smith and L. N. An, "Loop antennas for directive transmission into material half space," *Radio Sci.*, vol. 18, pp. 664–674, Sept.–Oct. 1983.

[9] J. S. Colburn and Y. Rahmat-Samii, "Electromagnetic scattering and radiation involving dielectric objects," *J. Electromagn. Waves Applicat.*, vol. 9, pp. 1249–1277, 1995.

[10] T. B. A. Senior, "Electromagnetic field penetration into a spherical cavity," *IEEE Trans. Electromagn. Compat.*, vol. EMC-16, pp. 205–208, Nov. 1974.

[11] R. W. Ziolkowski, D. P. Marsland, L. Libelo, and G. E. Pisane, "Scattering from an open spherical shell having a circular aperture and enclosing a concentric dielectric sphere," *IEEE Trans. Antennas Propagat.*, vol. 36, pp. 985–999, July 1988.

[12] H. P. Partal, J. R. Mautz, and E. Arvas, "Radiation from a circular loop near symmetrically placed conducting spherical caps," in *Proc. URSI Nat. Radio Sci. Meet.*, Boulder, CO, 1999, p. 255.

[13] H. P. Partal, E. Arvas, and J. R. Mautz, "Radiation from a circular loop in the presence of a dielectric sphere and/or a radome," in *Proc. USNC/URSI Radio Sci. Meet.*, Orlando, FL, 1999, p. 20.

[14] R. F. Harrington, *Time-Harmonic Electromagnetic Fields*. New York: McGraw-Hill, 1961.

[15] D. S. Jones, *The Theory of Electromagnetism*. New York: Pergamon, 1964.

[16] R. F. Harrington and J. R. Mautz, "An impedance sheet approximation for thin dielectric shells," *IEEE Trans. Antennas Propagat.*, vol. AP-23, pp. 531–534, July 1975.

Hakan P. Partal (S'92) was born in Malatya, Turkey, in 1970. He received the B.S.E.E. and M.S.E.E. degrees both from Yildiz Technical University, Istanbul, Turkey, in 1991 and 1995, respectively. He is currently working toward the Ph.D. degree as a Graduate Research Assistant in the area of electromagnetics at the Department of Electrical Engineering and Computer Science, Syracuse University, Syracuse, NY.

His current research interests include numerical electromagnetics, circular loops, and microwave circuits and devices.

Joseph R. Mautz (S'66–M'67–SM'75) was born in Syracuse, NY, in 1939. He received the B.S., M.S., and Ph.D. degrees in electrical engineering from Syracuse University, Syracuse, NY, in 1961, 1965, and 1969, respectively.

Until July 1993, he was a Research Associate in the Department of Electrical and Computer Engineering of Syracuse University, working on radiation and scattering problems. His primary fields of interest are electromagnetic theory and applied mathematics. He is presently affiliated with the Electrical and Computer Engineering Department, Syracuse University, but is not regularly employed there.

Ercument Arvas (M'85–SM'89) received the B.S. and M.S. degrees from METU, Ankara, Turkey, in 1976 and 1979, respectively, and the Ph.D. degree from Syracuse University, Syracuse, New York, in 1983, all in electrical engineering.

From 1984 to 1987, he was with the Electrical Engineering Department, Rochester Institute of Technology, Rochester, NY. He joined the Electrical Engineering and Computer Science Department, Syracuse University, in 1987, where he is currently a Professor. His research interests include numerical electromagnetics, antennas, and microwave circuits and devices.